Herschel-SPIRE, far-infrared properties of millimetre-bright and -faint radio galaxies

S. C. Chapman,[1]★ R. J. Ivison,[2,3] I. G. Roseboom,[4] R. Auld,[5] J. Bock,[6,7] D. Brisbin,[8]
D. Burgarella,[9] P. Chanial,[10] D. L. Clements,[11] A. Cooray,[12,6] S. Eales,[5]
A. Franceschini,[13] E. Giovannoli,[9] J. Glenn,[14] M. Griffin,[5] A. M. J. Mortier,[11]
S. J. Oliver,[4] A. Omont,[15] M. J. Page,[16] A. Papageorgiou,[5] C. P. Pearson,[17,18]
I. Pérez-Fournon,[19,20] M. Pohlen,[5] J. I. Rawlings,[16] G. Raymond,[5] G. Rodighiero,[13]
M. Rowan-Robinson,[11] Douglas Scott,[21] N. Seymour,[16] A. J. Smith,[4] M. Symeonidis,[16]
K. E. Tugwell,[16] M. Vaccari,[13] J. D. Vieira,[6] L. Vigroux,[15] L. Wang[4] and G. Wright[2]

[1]*Institute of Astronomy, University of Cambridge, Madingley Road, Cambridge CB3 0HA*
[2]*UK Astronomy Technology Centre, Royal Observatory, Blackford Hill, Edinburgh EH9 3HJ*
[3]*Institute for Astronomy, University of Edinburgh, Royal Observatory, Blackford Hill, Edinburgh EH9 3HJ*
[4]*Astronomy Centre, Department of Physics & Astronomy, University of Sussex, Brighton BN1 9QH*
[5]*Cardiff School of Physics and Astronomy, Cardiff University, Queens Buildings, The Parade, Cardiff CF24 3AA*
[6]*California Institute of Technology, 1200 East California Boulevard, Pasadena, CA 91125, USA*
[7]*Jet Propulsion Laboratory, 4800 Oak Grove Drive, Pasadena, CA 91109, USA*
[8]*Space Science Building, Cornell University, Ithaca, NY 14853-6801, USA*
[9]*Laboratoire d'Astrophysique de Marseille, OAMP, Université Aix-marseille, CNRS, 38 rue Frédéric Joliot-Curie, 13388 Marseille Cedex 13, France*
[10]*Laboratoire AIM-Paris-Saclay, CEA/DSM/Irfu - CNRS - Université Paris Diderot, CE-Saclay, pt courrier 131, F-91191 Gif-sur-Yvette, France*
[11]*Astrophysics Group, Imperial College London, Blackett Laboratory, Prince Consort Road, London SW7 2AZ*
[12]*Department of Physics & Astronomy, University of California, Irvine, CA 92697, USA*
[13]*Dipartimento di Astronomia, Università di Padova, vicolo Osservatorio, 3, 35122 Padova, Italy*
[14]*Department of Astrophysical and Planetary Sciences, CASA 389-UCB, University of Colorado, Boulder, CO 80309, USA*
[15]*Institut d'Astrophysique de Paris, UMR 7095, CNRS, UPMC Univ. Paris 06, 98bis boulevard Arago, F-75014 Paris, France*
[16]*Mullard Space Science Laboratory, University College London, Holmbury St. Mary, Dorking, Surrey RH5 6NT*
[17]*Space Science & Technology Department, Rutherford Appleton Laboratory, Chilton, Didcot, Oxfordshire OX11 0QX*
[18]*Institute for Space Imaging Science, University of Lethbridge, Lethbridge, Alberta T1K 3M4, Canada*
[19]*Instituto de Astrofísica de Canarias (IAC), E-38200 La Laguna, Tenerife, Spain*
[20]*Departamento de Astrofísica, Universidad de La Laguna (ULL), E-38205 La Laguna, Tenerife, Spain*
[21]*Department of Physics & Astronomy, University of British Columbia, 6224 Agricultural Road, Vancouver, BC V6T 1Z1, Canada*

ABSTRACT

We present the first study of the far-infrared (FIR) properties of high-redshift, radio-selected ultraluminous infrared galaxies (ULIRGs) using deep observations obtained with the Spectral and Photometric Imaging Receiver (SPIRE) from the *Herschel* Multi-tiered Extragalactic Survey (HerMES). These galaxies span a large range of 850-μm fluxes from submillimetre-luminous ∼10 mJy sources (SCUBA galaxies) to ∼1.5 mJy from stacked SCUBA non-detections, thus likely representing a complete distribution of ULIRG spectral energy distributions (SEDs). From Keck spectroscopic surveys in the Lockman-North field we identified a sample of 31 submillimetre galaxies (SMGs) and 37 submillimetre-faint, optically faint radio galaxies (OFRGs), all with radio-inferred IR luminosities $>10^{12}$ L$_\odot$. These galaxies were cross-identified with SPIRE 250-, 350- and 500-μm catalogues based on fluxes extracted at 24-μm positions in the SWIRE survey, yielding a sample of more than half of the

★E-mail: schapman@ast.cam.ac.uk

galaxies well detected in at least two of the SPIRE bandpasses. By fitting greybody dust models to the SPIRE photometry together with SCUBA 850-µm measurements (for OFRGs, only 850-µm upper limits), we infer dust temperatures and FIR luminosities. The OFRGs detected by SPIRE have median $\langle T_d \rangle = 41 \pm 5$ K and the SMGs have $\langle T_d \rangle = 34 \pm 5$ K, both in reasonable agreement with previous (pre-*Herschel*) estimates, reaffirming that the local FIR/radio correlation holds (at least for this subset of high-z ULIRGs) at high redshift (we measure $\langle q_{IR} \rangle = 2.43 \pm 0.21$ using S_{IR} derived from greybody fit coupled with a power-law extrapolation to the 24 µm). Our observations first confirm that a substantial fraction of OFRGs exhibits large infrared luminosities corresponding to SFRs of $\sim 400 \, M_\odot \, yr^{-1}$. The SPIRE observations secondly confirm the higher dust temperatures for these OFRGs than similarly selected SMGs, consistent with early predictions of the submillimetre-faint radio populations. Our observations also clearly confirm the large infrared luminosities of most SMGs selected with $S_{850 \, \mu m} > 5$ mJy and radio and strong 24-µm detections, corresponding to SFRs of $\sim 700 \, M_\odot \, yr^{-1}$.

Key words: galaxies: evolution – galaxies: high-redshift – galaxies: starburst.

1 INTRODUCTION

Submillimetre (submm) galaxies (SMGs – Smail, Ivison & Blain 1997) contribute significantly to the rapid build-up of stellar mass in the Universe at $z \sim 2$. SMGs have a typical redshift of $z \sim 2.2$ (Chapman et al. 2003a, 2004a, 2005; Wardlow et al. 2010), are massive systems ($M_* \sim 10^{10-11} \, M_\odot$; Swinbank et al. 2004; Greve et al. 2005; Tacconi et al. 2006) and are diverse in the extent and dynamics of their molecular gas reservoirs (e.g. Tacconi et al. 2008; Bothwell et al. 2010; Ivison et al. 2010b). Interferometric observations of SMGs' CO molecular gas suggest that the most luminous SMGs $S(850 \, \mu m) > 5$ mJy are merging systems (Engel et al. 2010) with high star formation efficiencies compared to typical galaxies of similar mass (Daddi et al. 2008). However, their selection at 850 µm is inherently biased towards colder dust ULIRGs, particularly at $z > 1$ (Eales et al. 2000; Blain et al. 2004). In particular, since submm observations probe the blackbody emission of dust in the Rayleigh–Jeans regime, they are anti-correlated with dust temperature ($S_{850} \propto T_{dust}^{-4.5}$)[1] for a given infrared (IR) luminosity, and galaxies with warmer dust can fall below the detection limit of current submm instruments. Recent work (e.g. Chapman et al. 2004b; Casey et al. 2009; Magnelli et al. 2010) has demonstrated that 850-µm-faint, high-redshift ULIRGs exist and may contribute significantly to the cosmic star formation rate density at its peak. These optically faint radio galaxies (OFRGs) are defined as radio sources having inferred ULIRG luminosities, with starburst (SB) or hybrid SB–AGN spectral features in the UV, and having 2.5σ limits on their submm fluxes which are consistent with them being fainter than 5 mJy at 850 µm. They have a comoving volume density (i.e. $\sim 10^{-5}$ Mpc^{-3} at $1 < z < 3$; Chapman et al. 2001, 2004b), stellar masses and radio sizes comparable to SMGs, and some have a dust temperature of ~ 52 K (Casey et al. 2009, 2010a). Studies of other IR-luminous galaxy populations both pre-*Herschel* (see Dey et al. 2008; Bussmann et al. 2009; Younger et al. 2009) and post-*Herschel* (see Magdis et al. 2010; Magnelli et al. 2010; Oliver et al. 2010; Roseboom et al. 2010) present even more evidence for diverse populations of luminous, dusty SBs at $z \gtrsim 1$.

However, sparse IR data, particularly in the 50–500 µm wavelength range, have limited the interpretation of the SMGs and OFRGs. Many of their fundamental properties still rely on indirect measurements. Direct determinations of SMG and OFRG dust temperatures are limited and have only been done using either a single rest-frame far-IR (FIR) point (SHARC-II/CSO observed 350 µm – Coppin et al. 2008; Kovacs et al. 2006, 2010) or with the most luminous examples of the population using the highly confused BLAST beam (250, 350 and 500 µm; Casey et al. 2010b; Chapin et al. 2010; Dunlop et al. 2010; Ivison et al. 2010a).

Observations of the rest-frame FIR emission of high-redshift galaxies with *Herschel* (Pilbratt et al. 2010) provide for the first time direct measurements of typical SMGs and OFRGs total IR luminosities and dust temperatures,[2] which are still highly debated (e.g. Swinbank et al. 2008; Dave et al. 2010). Importantly, they allow for tests of earlier measurements based on extrapolation from wavelengths either shortward or longerward of the FIR peak. Theoretical simulations of galaxy evolution continue to have difficulties in accounting for the inferred luminosities/star formation rates and number counts (Baugh et al. 2005; Narayanan et al. 2009; Dave et al. 2010). Open questions remain as to whether these luminosities have been overestimated or whether for instance the IMF is significantly more top heavy than in the local Universe (Baugh et al. 2005). In this Letter, we assess the *Herschel*-SPIRE properties of these two ULIRG populations selected using both submm and radio wavelengths. Calculations assume a flat, ΛCDM cosmology with $\Omega_\Lambda = 0.7$ and $H_0 = 71$ km s^{-1} Mpc^{-1}.

2 SAMPLE & OBSERVATIONS

The HerMES[3] Science Demonstration Phase (SDP) observations are detailed in table 1 of Oliver et al. (2010). We use deep Spectral and Photometric Imaging Receiver (SPIRE; Griffin et al. 2010) 250-, 350- and 500-µm observations of SMGs and OFRGs lying

---

[1] Since $L \propto M_d T^{5.5}$ while the Rayleigh–Jeans flux $S_{RJ} \propto M_d T$.

[2] Although for the hotter and lower redshift examples in our sample, PACS observations on the Wien side of the spectrum are required to truly constrain the dust temperature.

[3] http://hermes.sussex.ac.uk; Oliver et al. 2010 (in preparation)

in the Lockman-East (10^h51^{min}, +57) region (a subset of the larger Lockman-SWIRE field observations) obtained as part of this guaranteed time key programme in a key survey field having exquisite multiwavelength ancillary data. The radio/submm sources lie within a subfield covered by a deep VLA 1.4 GHz radio pointing, within a region of 15×15 arcmin^2 (Ibar et al. 2009). Flux densities are measured using a PSF fitting technique based on cross-identifed (XID) prior sources positions detected at 24 μm (Roseboom et al. 2010), which accounts for blending of SPIRE source fluxes by simultaneous fitting to multiple sources. All sources in our fields are essentially point sources at the resolution of *Herschel*. The association between the *Spitzer*-IRAC and MIPS and SPIRE sources is thus facilitated by the use of these priors. The quality of the SPIRE 250-, 350- and 500-μm catalogues has been estimated using Monte Carlo simulations (photometry error, completeness and contamination as a function of the flux density). In the Lockman-East field our observations have average 1σ XID source extraction errors of 3.6, 4.2 and 4.8 mJy at 250, 350 and 500 μm, respectively, and the confusion noise is quoted as 5.8, 6.3 and 6.8 mJy beam^{-1} rms, respectively, by Nguyen et al. (2010), which we apply in quadrature to the flux errors.

Some SMGs and OFRGs have previously been studied spectroscopically in Lockman-East in several works (Chapman et al. 2003a, 2004b, 2005; Ivison et al. 2005; Casey et al. 2009, 2010). The parent sample for this study consists of a sample of 376 radio sources with spectroscopic follow-up in the Lockman-East field. For this initial foray into the SPIRE properties of luminous, high-z radio sources, we impose a $>5\sigma$ 24-μm detection threshold (from the SWIRE catalogue – Lonsdale et al. 2004) in order to extract the SPIRE fluxes at that position. This removes some of the confusion issues arising in the full radio source sample, although it brings some bias to the study. We adopt a catalogue based on a 24-μm prior, as opposed to a radio prior, as we have uniform 24-μm coverage across these areas and a clear understanding of the effect of this input list on the data. Future contributions will include a broader radio prior catalogue to further explore these populations. This catalogue consists of 140 sources. We further restrict this sample to those with radio luminosities $>4.5 \times 10^{30}$ erg s^{-1} Hz^{-1}, corresponding to an equivalent ULIRG FIR luminosity ($>10^{12}$ L$_\odot$) assuming the radio-FIR correlation (e.g. Condon, Anderson & Helou 1991), resulting in a sample of 68 sources.

The final sample consists of 31 securely identified SMGs and 37 OFRGs with IR luminosities $>10^{12}$ L$_\odot$, and which are cross-matched with our SPIRE 250-, 350- and 500-μm multiwavelength catalogues based on sources extraction using prior detections at 24 μm. 19 of the SMGs and 21 of the OFRGs in our sample are detected in at least two of the SPIRE bandpasses and form the sample we focus on in this work. The SMGs have an average (de-boosted using the Coppin et al. 2006 counts and method) $S_{850\,\mu m} = 6$ mJy, while the OFRGs have average $S_{850\,\mu m} = 1.5$ mJy (which we have not attempted to deboost here), together likely representing a complete distribution of ULIRG SEDs. In Fig. 1 we plot the average SEDs of SMGs and OFRGs which is constructed by redshifting each template fit to the rest frame, and interpolating observed data points at the average redshift of the sample. The dispersion in the average SED is comparable to the individual flux errors combined with confusion noise. Fig. 1 also compares the Dale & Helou SED templates ranging from 25 to 45 K, and an average SMG template from Pope et al. (2008). Fig. 3 shows the redshift distribution and Table S1 lists the galaxies' properties.
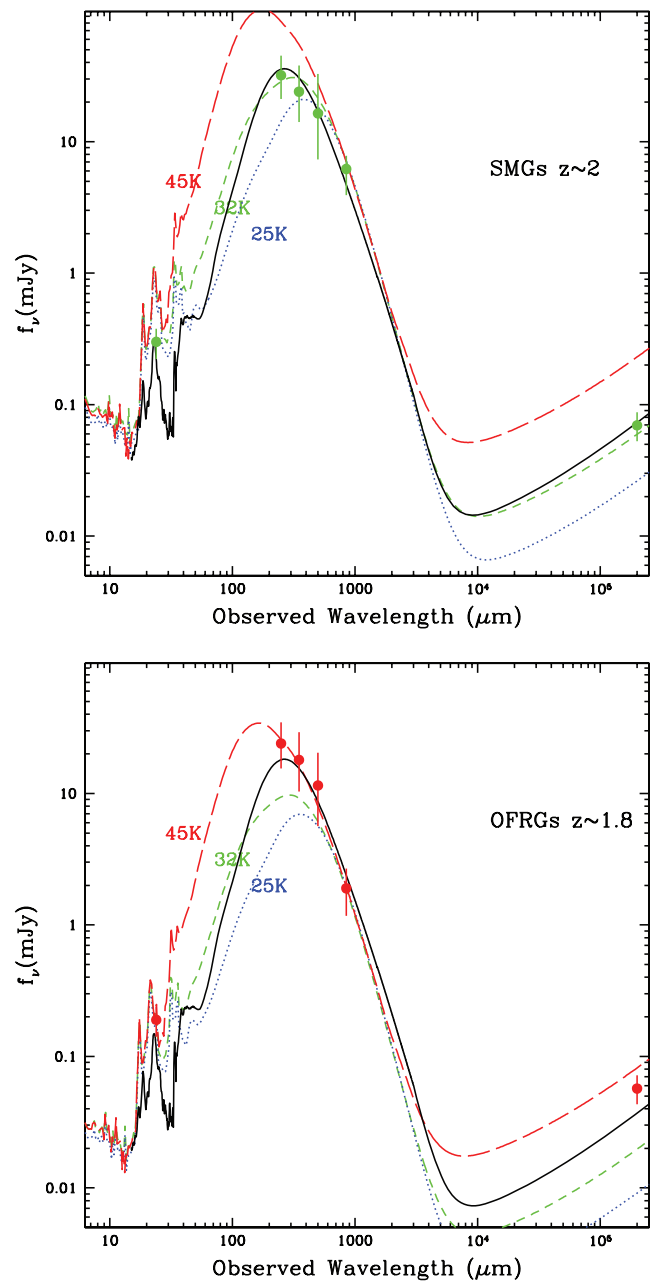
Figure 1. Average SEDs of SMGs (top panel) and OFRGs (bottom panel), after redshifting each template fit to the rest frame, and interpolating observed data points at the average redshift of the sample. Circles present our SPIRE measurements, SCUBA 850 μm and VLA 1.4-GHz data. Error bars show the dispersion in the sample, which is comparable to the individual flux errors combined with confusion noise. Red, green and blue lines (segment, dashed and dotted) present the Dale & Helou SED templates from 25 to 45 K. An average SMG template from Pope et al. (2008) is also overlaid as solid black line.

3 RESULTS

We fit the SPIRE (250, 350 and 500 μm) and SCUBA (850 μm; only the upper limit in the case of the OFRGs) flux densities to FIR dust models (see Figs 1 and 2). The model assumes a modified blackbody emission curve, in the optically thin approximation, with
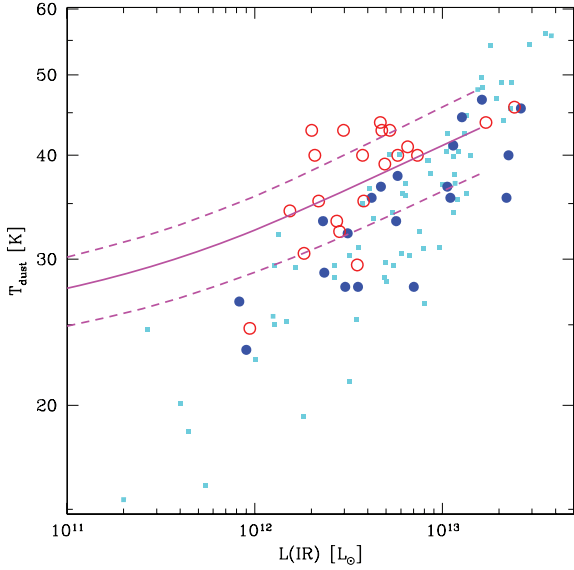
Figure 2. The dust temperature–luminosity relation. Filled blue/empty red circles are from our SMGs/OFRGs Lockman-East sample. Temperature uncertainties range from 3 to 7 K (depending on how well the peak is sampled), while luminosity uncertainties are ∼0.2 dex (given the power-law extrapolation down the Wien-side model fit). The cyan squares represent results for SMGs extrapolated by Chapman et al. (2005) from radio and submm data. The Chapman et al. (2003b) derivation of the median and interquartile range of the T_d–L_{IR} relation observed locally is shown by solid and dot–dashed lines, linearly extrapolated to 10^{13} L$_\odot$.

a single dust temperature:

$$S_\nu \propto \frac{\nu^{3+\beta}}{\exp(h\nu/kT_d) - 1}, \tag{1}$$

where S_ν, the flux density, is a function of rest frequency ν, the emissivity β, dust temperature T_d, and FIR luminosity L_{FIR} (which governs the normalization of the function). Their total IR luminosities (L_{IR}[8–1000 μm]) are inferred from these best fits using the FIR luminosity definition (L_{FIR}[40–120 μm]) given by Helou et al. (1988) and a colour-correction term (Dale et al. 2001; L_{IR} = $1.91 \times L_{FIR}$). The model fixes emissivity to $\beta = 1.5$. The model has T_d and L_{IR} as free parameters. While the luminosities here are clearly an approximation to the true L_{IR}, we leave a more detailed estimation to the availability of shorter wavelength *Herschel* data. We choose to make this model rigid since the flux errors are known to be correlated, which reduces the effective number of degrees of freedom.

This single dust temperature characterization provides a good description of the SMGs and OFRGs FIR SED; however for seven SMGs and nine OFRGs, this single dust temperature model yields high χ^2 values. All these galaxies appear either to be the less luminous examples, exhibit FIR colours possibly suggestive of hotter systems, or may simply lie in confused regions. However, given the extreme dust masses (∼10^9 M$_\odot$) of SMGs, one should expect optical depths to matter, especially in the shorter wavelength SPIRE bands. Assuming typical emission scales of ∼2 kpc, we expect optical depths of 1–2 in the 250- and 350-μm bands for a $z \sim 2$ SMG (see Kovacs et al. 2010). While the effect is still moderate such that the optically thin approximation is crudely correct, the high χ^2 found for some of the galaxies may be an indication of the shortcoming of the single temperature, optically thin model.

Our results appear to be relatively insensitive to β and to the single dust component model; with $\beta = 2$, the differences in T_d

are $\Delta T_d \pm 3$ K. In addition, the multiple dust components model of Dale & Helou (2002) yields rest-frame IR colours ($S_{60\,\mu m}/S_{100\,\mu m}$), or equivalently T_d, which are in reasonable agreement with those inferred from our greybody analysis. In Fig. 1, we also overplot a composite SMG spectrum, from Pope et al. (2008), normalized to 24-μm flux density.

The T_d–L_{IR} plane forms an important diagnostic for assessing the properties of luminous IR galaxies and their spectral shapes. In Fig. 2, the locations of our SMGs and OFRGs on the T_d–L_{IR} plane are shown. These estimates are amongst the first direct observational measurements of the dust temperatures and the IR luminosities of OFRGs. Previous studies with SHARC-II and BLAST have attempted similar analyses mainly on SMGs with caveats presented in Section 1 (Kovacs et al. 2006, 2010; Coppin et al. 2008; Amblard et al. 2010; Casey et al. 2010; Chapin et al. 2010; Dunlop et al. 2010; Ivison et al. 2010a). Our observations suggest that high-redshift ULIRGs show a wide range of dust temperatures. At intermediate IR luminosities of ULIRGs [$L_{IR} \sim (3-5) \times 10^{12}$ L$_\odot$], the dust temperature dispersion observed in our sample might suggest a higher T_d–L_{IR} scatter than that deduced from local IRAS galaxies by Chapman et al. (2003b) and Chapin, Hughes & Aretxaga (2009). OFRGs tend to be biased towards hotter dust temperatures, with median $\langle T_d \rangle = 41 \pm 5$ K (quoting standard deviations of the sample) and $\langle L_{IR} \rangle = 3.8 \times 10^{12}$ L$_\odot$, while SMGs appear to have lower dust temperatures with median $\langle T_d \rangle = 34 \pm 5$ K and $\langle L_{IR} \rangle = 7.1 \times 10^{12}$ L$_\odot$. There is a trend of increasing T_d with increasing L_{IR} for both SMGs and OFRGs. First the $S_{850\,\mu m}$ selection effectively selects $M_d \times T_d$, thus for a given mass warmer galaxies are favoured, which will be more luminous. Secondly, we expect something of a T–L correlation because of the temperature bias in our luminosity estimates (see below).

In Fig. 3, we depict the locations of SMGs and OFRGs on the $S(850\,\mu m)$–z and –L_{IR} planes. The weak correlations between $S(850\,\mu m)$ and L_{IR} (suggested by Pope et al. 2005) are rendered meaningless when the sample of OFRGs are considered together
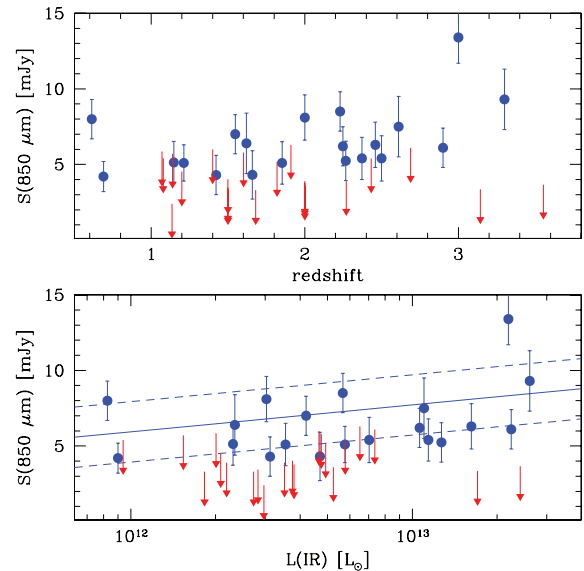
Figure 3. Submm flux densities as function of the redshift and FIR luminosity, revealing both the redshift distribution of our sample and the range in 850-μm fluxes probed for two samples which have similar average radio fluxes. Symbols are same as in Fig. 2 except the OFRGs for which we have only upper limits (flux + 2σ). Solid and dashed lines show the linear fit to the $S_{850\,\mu m}$–L_{IR} relation for SMGs and the 1σ envelope.

with SMGs. Selection effects are a concern in these diagrams since our focus on submm-bright or submm-faint radio sources with relatively bright 24-μm detections, as well as SPIRE detections, means that we may have missed populations of galaxies which would fill in and further elucidate these trends.

4 DISCUSSION

Comparing to previous studies of SMG dust temperatures, Chapman et al. (2005) found $T_d = 36 \pm 7$ K by using the FIR/radio correlation (e.g. Condon et al. 1991). As mentioned earlier, these measurements relied on indirect indicators of T_d. In order to more directly compare our SPIRE results with previous studies, we applied the method of Chapman et al. (2005) to our SMG sample, using only the radio and 850-μm data and fitting Dale & Helou (2002) dust SED templates. T_d is then derived by applying a mapping from their $S_{60\,\mu m}/S_{100\,\mu m}$. Using the full SED information for these SPIRE sources, we find that T_d, measured from S_{850} and $L_{1.4\,GHz}$ alone, overestimates the dust temperature by 2 ± 2 K for SMGs, and on average overestimates the dust temperature of OFRGs by 7 ± 4 K. This is remarkable agreement, given the scatter in the IR–radio relation and poorly defined 850-μm fluxes for individual OFRGs. Kovacs et al. (2006) observed 21 SMGs at 350 μm and measured FIR luminosities independent of radio luminosity using FIR data ranging from observed 350 to 1200 μm. They found that the local FIR/radio correlation overestimates FIR luminosity by factors of ∼0.2–0.4 dex for SMGs, which agrees with our SPIRE analysis.

To demonstrate these discrepancies more clearly, we estimate the bolometric q_{IR}, the ratio of IR-integrated flux to radio flux, as described in Ivison et al. (2010c):

$$q_{IR} = \log\left(\frac{S_{IR}}{3.75 \times 10^{12}\,W\,m^{-2}}\right) - \log\left(\frac{S_{1.4\,GHz}}{W\,m^{-2}\,Hz^{-1}}\right), \quad (2)$$

where S_{IR} taken from rest frame 8 to 1000 μm as described before and the radio flux density $S_{1.4\,GHz}$ is K-corrected, assuming a radio slope, $\alpha = 0.75$ (Ibar et al. 2010). We note, however, that the choice of radio spectral slope only affects the q_{IR} ratio by <10 per cent. We also note that the Dale & Helou SED templates assume a FIR/radio correlation with an effective $\langle q_{IR} \rangle = 2.62$ (Yun, Reddy & Condon 2001).[4] Since our S_{IR} estimates are based on the greybody fits, we extrapolate from the peak to the 24-μm point with an appropriate power law, yielding $\langle q_{IR} \rangle = 2.43 \pm 0.2$, thereby suggesting a reliable estimate of the IR luminosity of $z \sim 2$ ULIRGs can be obtained from their radio luminosity using a similar q to that inferred locally, as inferred in Kovacs et al. (2006, 2010).

While the SMG composite template (Pope et al. 2008) used in Fig. 1 is carefully derived based on mid-IR to FIR data of SMGs to date, it fails to fit the SPIRE FIR data of this sample well. In some cases, it under/overestimates the FIR luminosities by ±0.5 dex. This illustrates how a 24-μm-normalized SED fitting procedure, which is common in the literature (Desai et al. 2009), places poor constraints on the breadth of FIR properties of ULIRG samples, especially in the absence of direct FIR measurements. Similarly, the use of the 24-μm emission and of the Chary & Elbaz SED library yields an inaccurate estimate of the IR luminosity characterized by a large

[4] The Helou et al. (1988) definition of 'q' using $L[40–120\,\mu m]$ differs from our adopted Ivison et al. (2010a) definition of q_{IR} with $L[8–1000\,\mu m]$, all other terms being the same. Thus with an average colour conversion of 1.91, we find $q_{IR} \sim q + 0.28$.

scatter (∼0.5 dex) and a systematic overestimation (∼2×) in the luminosities of ULIRGs. For radio ULIRGs under investigation here, luminosity extrapolations based on the radio emission are considerably more reliable than those based on the mid-IR emission (e.g. Elbaz et al. 2010, although they have shown that 24 μm is a good representation of L_{IR} for lower redshift galaxies).

It is of interest to estimate the expected IR luminosities of our SPIRE-undetected SMGs and OFRGs, although in the latter case there is some likelihood that an AGN is boosting the radio luminosity. The SPIRE non-detections of SMGs are generally found to be consistent with the properties inferred from the detections. We use $\langle q_{IR} \rangle = 2.43$ and apply the Dale & Helou SED templates normalized to these IR luminosities. For the SMGs we find that for five out of 11 undetected SMGs, SPIRE flux densities inferred using these fits lie below the detection threshold. Of the six sources with predictions for SPIRE fluxes above the detection threshold, three have evidence in the UV spectra for AGN contributions. For the OFRGs the lack of 850-μm detection and SPIRE detections makes it likely that an AGN is generating the radio luminosity.

The main concern with this study is just how representative the sample of ULIRGS is to the wider SMG and OFRG populations given the use of a 24-μm prior. The 24-μm detection could favour those galaxies that are either warmer or have larger fractions of warm ($T > 35$ K) gas than average, biasing both the luminosities and temperatures. Apart from misrepresenting the class of objects as a whole, the different temperature distributions also question the usability of local templates (which presumably have a more average temperature distribution). Also, because the 24-μm band falls into a range of the rest-frame spectrum where there are a lot of aromatic features, it is even more complicated to assess what subclasses are selected at what redshift. While our study has some clear advantages compared to prior FIR studies of SMGs and OFRGs, the additional bias is a disadvantage, motivating a more thorough investigation of the SPIRE properties of more complete samples.

Our observations first confirm that a substantial fraction of OFRGs (∼50 per cent of the 24-μm XID SPIRE sample) exhibits large IR luminosities corresponding to SFRs of 380 $M_\odot$ yr^{-1} (SFR [$M_\odot$ yr^{-1}] = $1 \times 10^{-10} L_{IR}$ [$L_\odot$], assuming a Chabrier IMF). The complicated selection of our sample in this study, including the required 24-μm XID prior for SPIRE flux extraction, means that a precise volume density for these IR-luminous OFRGs is not trivial to estimate. As a lower limit, given the OFRGs without 24-μm XID prior which have yet to be studied with *Herschel*, the IR-luminous OFRGs are about one-fourth as numerous as equivalent luminosity SMGs at $z \sim 2$, or >7×10^{-6} Mpc^{-3} for $L_{IR} = 2$–$6 \times 10^{12} L_\odot$. The SPIRE observations secondly confirm the higher dust temperatures for these OFRGs than similarly selected SMGs with SPIRE observations, consistent with our early predictions of the submm-faint radio populations. Understanding the different dust temperatures and the connections to SMGs is possible if we take the luminosities of SMGs as dominated by star formation, as for OFRGs even if an AGN contribution cannot be ruled out. Since $L \propto M_d T^{5.5}$, warmer dust implies less dust. As such, given the similar SMG and OFRG luminosities, but their different typical temperatures, a possible conclusion is simply that OFRGs have about a third of the dust content relative to stellar mass. This would naturally suggest that OFRGs are simply a different phase of the SB than the cooler SMGs. Either OFRGs are an earlier phase, before the full-scale build-up of dust mass, or a later phase, where much of the dust is blown out by superwinds or consumed by a central black hole.

Our observations also clearly confirm the remarkably large IR luminosities of most SMGs ($S_{850\,\mu m} > 5$ mJy) which correspond to

SFRs of $710 \, \mathrm{M_\odot \, yr^{-1}}$. The remaining 12 SMGs in our Lockman-East catalogue which are not found in the XID SPIRE catalogue do not distinguish themselves in terms of 850 or 24-μm fluxes. Although their radio 850-μm inferred T_d is cooler on average than those presented here, it is likely source confusion in the SPIRE maps which limits their study. More detailed evolutionary understanding of high-z ULIRGs will be facilitated by future studies of deep *Herschel* observations and including the shorter wavelength bands.

REFERENCES

Amblard A. et al., 2010, A&A, 518, L9
Baugh C. M. et al., 2005, MNRAS, 356, 1191
Blain A. W., Chapman S. C., Smail I., Ivison R., 2004, ApJ, 611, 52
Bothwell M. S. et al., 2010, MNRAS, 405, 219
Bussmann R. S. et al., 2009, ApJ, 705, 184
Casey C. M. et al., 2009, MNRAS, 399, 121
Casey C. M. et al., 2010a, MNRAS, submitted (arXiv:0910.5756)
Casey C. M., Chapman S. C., Smail I., Alaghband-Zadeh S., Bothwell M. S., Swinbank A. M., 2010b, MNRAS, in press (arXiv:1009.5709)
Chapin E., Hughes D., Aretxaga I., 2009, MNRAS, 393, 653
Chapin E. et al., 2010, MNRAS, submitted (arXiv:1003.2647)
Chapman S. C. et al., 2001, ApJ, 548, L147
Chapman S. C., Blain A., Ivison R., Smail I., 2003a, Nat, 422, 695
Chapman S. C., Helou G., Lewis G. F., Dale D., 2003b, ApJ, 588, 186
Chapman S. C., Smail I., Windhorst R., Muxlow T., Ivison R. J., 2004a, ApJ, 611, 732
Chapman S. C., Smail I., Blain A., Ivison R. J., 2004b, ApJ, 614, 671
Chapman S. C., Blain A. W., Smail I., Ivison R., 2005, ApJ, 622, 772
Condon J. J., Anderson M. L., Helou G., 1991, ApJ, 376, 95
Coppin K. et al., 2006, MNRAS, 372, 1621
Coppin K. et al., 2008, MNRAS, 378, 214
Daddi E. et al., 2008, ApJ, 628, 50
Dale D. A., Helou G., 2002, ApJ, 576, 159
Dale D. et al., 2001, ApJ, 562, 142

Dave R., Finlator K., Oppenheimer B. D., Fardal M., Katz N., Keres D., Weinberg D. H., 2010, MNRAS, 404, 1355
Desai V. et al., 2009, ApJ, 677, 943
Dey A. et al., 2008, ApJ, 677, 943
Dunlop J. et al., 2010, MNRAS, doi:10.1111/j.1365-2966.2010.17278.x
Eales S. et al., 2000, AJ, 120, 2244
Elbaz D. et al., 2010, A&A, 518, L29
Engel H. et al., 2010, ApJ, in press (arXiv:1009.2495)
Greve T. et al., 2005, ApJ, 621, 124
Griffin M. et al., 2010, A&A, 518, L3
Helou G., Khan I. R., Malek L., Boehmer L., 1988, ApJS, 68, 151
Ibar E. et al., 2009, MNRAS, 397, 281
Ibar E. et al., 2010, MNRAS, 401L, 53
Ivison R. J. et al., 2005, MNRAS, 364, 1025
Ivison R. J. et al., 2010a, MNRAS, 402, 245
Ivison R. J. et al., 2010b, MNRAS, 404, 198
Ivison R. J. et al., 2010c, A&A, 518, L31
Kovacs A. et al., 2006, ApJ, 634, 31
Kovacs A. et al., 2010, ApJ, 717, 29
Lonsdale C. et al., 2004, ApJS, 154, 54
Magdis G. E. et al., 2010, MNRAS, in press (arXiv:1007.4900)
Narayanan D., Cox T. J., Hayward C. C., Younger J. D., Hernquist L., 2009, MNRAS, 400, 1919
Nguyen H. T. et al., 2010, A&A, 518, L5
Oliver S. et al., 2010, A&A, 518, L21
Pilbratt G. et al., 2010, A&A, 518, L1
Pope A., Borys C., Scott D., Conselice C., Dickinson M., Mobasher B., 2005, MNRAS, 358, 149
Pope A. et al., 2008, ApJ, 603, L13
Roseboom I. et al., 2010, MNRAS, in press (arXiv:1009.1658)
Smail I., Ivison R., Blain A., 1997, ApJ, 490, L5
Swinbank A. M., Smail I., Chapman S. C., Blain A. W., Ivison R. J., Keel W. C., 2004, ApJ, 617, 64
Swinbank A. M. et al., 2008, MNRAS, 391, 420
Tacconi L. J. et al., 2006, ApJ, 640, 228
Tacconi L. J. et al., 2008, ApJ, 680, 246
Wardlow J. et al., 2010, MNRAS, in press (arXiv:1006.2137)
Younger J. D. et al., 2009, MNRAS, 394, 1685
Yun M. S., Reddy N. A., Condon J. J., 2001, ApJ, 554, 803

SUPPORTING INFORMATION

Additional Supporting Information may be found in the online version of this article:

Table S1. The properties of the SMGs and SFRGs with detected SPIRE fluxes from the XID-24 μm sample. Positions are *Spitzer*-24 μm positions, and redshifts are derived from Keck rest-frame-UV spectra unless otherwise noted. Separation notes the distance of the SPIRE 250 μm source from the 24 μm centroid. L_FIR and T_D are derived from multiwavelength fits as described in the text.

Please note: Wiley-Blackwell are not responsible for the content or functionality of any supporting materials supplied by the authors. Any queries (other than missing material) should be directed to the corresponding author for the article.

This paper has been typeset from a TEX/LATEX file prepared by the author.